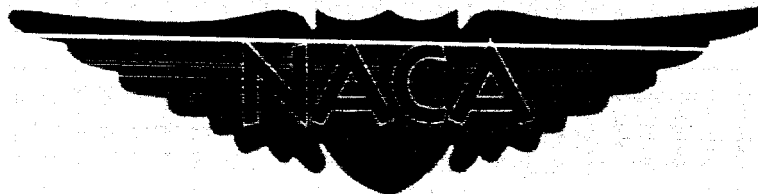# RESEARCH MEMORANDUM

PRELIMINARY INVESTIGATION OF DYNAMIC LATERAL STABILITY

CHARACTERISTICS OF A CONFIGURATION OF TH

AMERICAN X-15 RESEARCH AIRPLANE

By Martin T. Moul

Langley Aeronautical Laboratory
Langley Field, Va.

DECLASSIFIED - EFFECTIVE 1-15-64
Authority: Memo Geo. Drobka NASA HQ.
Code ATSS-A Dtd. 3-12-64 Subj: Change
in Security Classification Markings.

GPO PRICE $

OTS PRICE(S) $

Hard copy (HC)   2.00

Microfiche (MF)   .50

NATIONAL ADVISORY COMMITTEE
FOR AERONAUTICS

WASHINGTON
February 8, 1957
Reclassified December 3, 1958

NATIONAL ADVISORY COMMITTEE FOR AERONAUTICS

RESEARCH MEMORANDUM

PRELIMINARY INVESTIGATION OF DYNAMIC LATERAL STABILITY

CHARACTERISTICS OF A CONFIGURATION OF THE NORTH

AMERICAN X-15 RESEARCH AIRPLANE

By Martin T. Moul

SUMMARY

A preliminary theoretical investigation has been made to determine the dynamic lateral stability characteristics of a configuration of the North American X-15 research airplane. Of specific concern were characteristic modes, period and damping, airplane response to yaw and roll controls, ratio of roll to sideslip in the Dutch-roll oscillation, and the roll-coupling problem.

Results are presented for a Mach number of 6.86, altitudes of 100,000, 150,000, and 200,000 feet, and angles of attack of $0°$ and $16°$. Configurations with speed brakes closed and fully open were investigated and two intermediate cases, which may represent partially opened speed brakes, were also included. Roll-coupled motions were noted for an altitude of 100,000 feet with either yaw or roll controls operative. Large roll-to-sideslip ratios, rolling sensitivity to yaw inputs, and roll coupling resulting from yaw inputs were noted for an angle of attack of $0°$ and could be alleviated by reducing the effective dihedral C_{l_β}.

INTRODUCTION

A program has been initiated at the Langley Laboratory to investigate analytically the dynamic stability and controllability of the North American X-15 research airplane for the proposed flight plans. Dynamic longitudinal and lateral stability characteristics, response of the airplane to control inputs, and ability of a pilot to control the airplane will be investigated in the program.

A preliminary study has been made to determine the nature of the dynamic lateral behavior of the airplane at high speeds and altitudes where aerodynamic damping is poor. Aerodynamic characteristics of the airplane obtained from tests in the Langley 11-inch hypersonic tunnel

for two speed-brake positions were utilized. In addition two other com-
binations of C_{n_β} and C_{l_β}, which may represent some other brake posi-
tions, were selected.

Conditions of the investigation are a Mach number of 6.86, altitudes
of 100,000, 150,000, and 200,000 feet, and angles of attack of 0° and 16°.
Results presented are period and damping of the lateral modes, roll-to-
sideslip ratio, and three- and five-degree-of-freedom responses to rolling-
and yawing-moment inputs.

SYMBOLS

A,B,C,D	coefficients of lateral-stability characteristic equation
$-a \pm i\omega$	complex roots of lateral-stability characteristic equation
b	wing span, ft
C_W	weight coefficient, $\dfrac{W}{qS}$
C_l	rolling-moment coefficient, $\dfrac{\text{Rolling moment}}{qSb}$
C_n	yawing-moment coefficient, $\dfrac{\text{Yawing moment}}{qSb}$
C_Y	side-force coefficient, $\dfrac{\text{Side force}}{qS}$
h_p	altitude, ft
I_X	moment of inertia about principal X-axis, slug-ft^2
I_Y	moment of inertia about principal Y-axis, slug-ft^2
I_Z	moment of inertia about principal Z-axis, slug-ft^2
K_X	nondimensional radius of gyration in roll about stability X-axis, $\sqrt{K_{X_0}^2\cos^2\eta + K_{Z_0}^2\sin^2\eta}$
K_{X_0}	nondimensional radius of gyration in roll about principal X-axis, $\sqrt{I_X/mb^2}$

K_Z nondimensional radius of gyration in yaw about stability Z-axis, $\sqrt{K_{Z_O}^2\cos^2\eta + K_{X_O}^2\sin^2\eta}$

K_{Z_O} nondimensional radius of gyration in yaw about principal Z-axis, $\sqrt{I_Z/mb^2}$

K_{XZ} nondimensional product-of-inertia parameter, $\left(K_{X_O}^2 - K_{Z_O}^2\right)\sin\eta\cos\eta$

M Mach number

m mass, slugs

P period of oscillation, sec

p rolling velocity, radians/sec

q pitching velocity, radians/sec or dynamic pressure, $\frac{1}{2}\rho V^2$, lb/sq ft

r yawing velocity, radians/sec

S wing area, sq ft

$T_{1/2}$ time to damp to one-half amplitude, sec

W weight, lb

V airspeed, ft/sec

α angle of attack, radians

β angle of sideslip, radians

γ inclination of flight path to horizontal, deg

δ_a aileron deflection, deg

δ_r rudder deflection, deg

ϵ angle between body axis and principal axis, deg

η inclination of principal X-axis of airplane with respect to flight path, deg

λ root of lateral-stability characteristic equation

μ_b relative density factor, $m/\rho Sb$

ρ mass density of air, slugs/cu ft

ϕ angle of bank, radians

ψ angle of yaw, radians

Derivatives:

$$C_{Y_\beta} = \frac{\partial C_Y}{\partial \beta}, \text{ per radian}$$

$$C_{n_\beta} = \frac{\partial C_n}{\partial \beta}, \text{ per radian}$$

$$C_{l_\beta} = \frac{\partial C_l}{\partial \beta}, \text{ per radian}$$

$$C_{l_p} = \frac{\partial C_l}{\partial \frac{pb}{2V}}, \text{ per radian}$$

$$C_{n_p} = \frac{\partial C_n}{\partial \frac{pb}{2V}}, \text{ per radian}$$

$$C_{l_r} = \frac{\partial C_l}{\partial \frac{rb}{2V}}, \text{ per radian}$$

$$C_{n_r} = \frac{\partial C_n}{\partial \frac{rb}{2V}}, \text{ per radian}$$

$$C_{l_{\delta_a}} = \frac{\partial C_l}{\partial \delta_a}, \text{ per deg}$$

$$C_{n_{\delta_r}} = \frac{\partial C_n}{\partial \delta_r}, \text{ per deg}$$

Subscripts:

o   initial value

crit   critical value

AIRPLANE DESCRIPTION

A three-view drawing of the airplane is given in figure 1 and the geometric and inertia characteristics pertinent to this study, in table I.

For this investigation, the yaw and roll reaction controls of the airplane were assumed to be in use. The roll control produces 17 pounds thrust and a rolling moment of 120 foot-pounds, and the yaw control produces 90 pounds thrust and a yawing moment of 2,275 foot-pounds. For altitudes of 100,000 and 200,000 feet, the moment coefficients of the reaction controls, control-effectiveness estimates for the airplane aerodynamic controls, and the equivalent aerodynamic-control deflections are given in the following table. These equivalent aerodynamic-control deflections are valid for the conditions that the ailerons and rudder produce no cross or coupling moments.

Altitude, ft	C_n	$C_{n_{\delta_r}}$	Rudder deflection, deg	C_l	$C_{l_{\delta_r}}$	Aileron deflection, deg
100,000	-0.00068	-0.0017	0.4	-0.000036	-0.00036	0.1
200,000	-.035	-.0017	20	-.00184	-.00036	5

Reaction controls are intended as alternate controls for use at low dynamic pressures where aerodynamic controls are ineffective. The equivalent aerodynamic-control deflections in the preceding table indicate that rudder and aileron would be in use at an altitude of 100,000 feet, whereas reaction controls would be used at 200,000 feet.

Data from model tests of a configuration of the North American X-15 research airplane in the Langley 11-inch hypersonic tunnel are presented in figure 2 for two speed-brake configurations, brakes closed and open 45° (configurations 1 and 4, respectively). Since the brakes-closed configuration is directionally unstable, two other values of C_{n_β} and C_{l_β} were selected for the purpose of this analysis and may represent two intermediate brake configurations (configurations 2 and 3). The

sideslip derivatives of the test models and the two selected intermediate brake configurations are summarized in table II for angles of attack of $0°$ and $16°$.

ANALYSIS

Characteristic Equation

In this investigation an altitude range (100,000 to 200,000 feet) was selected for which aerodynamic damping was expected to be poor and rotary derivatives could be neglected. Under these conditions a pilot will experience unusual difficulty in controlling the airplane.

The lateral equations of motion for a stability-axes system are, when rotary derivatives are neglected,

$$
\left.
\begin{aligned}
2\mu_b\left(\frac{b}{V}\right)^2 K_X{}^2\ddot{\phi} - 2\mu_b\left(\frac{b}{V}\right)^2 K_{XZ}\ddot{\psi} &= C_{l_\beta}\beta + C_l \\[2mm]
2\mu_b\left(\frac{b}{V}\right)^2 K_Z{}^2\ddot{\psi} - 2\mu_b\left(\frac{b}{V}\right)^2 K_{XZ}\ddot{\phi} &= C_{n_\beta}\beta + C_n \\[2mm]
2\mu_b\left(\frac{b}{V}\right)\dot{\psi} + 2\mu_b\left(\frac{b}{V}\right)\dot{\beta} &= C_{Y_\beta}\beta + C_W\cos\gamma + \left(C_W\sin\gamma\right)\psi
\end{aligned}
\right\}
\tag{1}
$$

The characteristic equation is

$$
8\mu_b{}^3\left(\frac{b}{V}\right)^3\left(K_X{}^2 K_Z{}^2 - K_{XZ}{}^2\right)\lambda^3 - 4\mu_b{}^2\left(\frac{b}{V}\right)^2 C_{Y_\beta}\left(K_X{}^2 K_Z{}^2 - K_{XZ}{}^2\right)\lambda^2 +
$$

$$
4\mu_b{}^2\left(\frac{b}{V}\right)\left(K_X{}^2 C_{n_\beta} + K_{XZ}C_{l_\beta}\right)\lambda - 2\mu_b C_W\cos\gamma\left(K_Z{}^2 C_{l_\beta} + K_{XZ}C_{n_\beta}\right) = 0
\tag{2}
$$

The modes represented by equation (2) are an oscillatory (Dutch roll) mode and an aperiodic mode. By comparison with the general lateral-stability characteristic equation obtained when rotary derivatives are included, it is seen that the normal spiral root is zero for this simplified condition. The aperiodic root obtained for the simplified condition is related to the usual damping-in-roll mode but is much smaller because C_{l_p} is assumed to be equal to zero.

Approximations to the Roots

The characteristic roots may be quickly and accurately determined from approximate factors of the characteristic equation when rotary derivatives are neglected. The general characteristic equation

$$A\lambda^3 + B\lambda^2 + C\lambda + D = 0 \tag{3}$$

can be written as

$$A(\lambda - \lambda_1)\left[(\lambda + a)^2 + \omega^2\right] = 0$$

where λ_1 and $(-a \pm i\omega)$ are the actual roots. The approximations to the roots are

$$\left.\begin{aligned}
\lambda_1 &= \frac{C_W \cos \gamma}{2\mu_b \frac{b}{V}} \frac{\left(K_Z^2 C_{l_\beta} + K_{XZ} C_{n_\beta}\right)}{\left(K_X^2 C_{n_\beta} + K_{XZ} C_{l_\beta}\right)} \\[2em]
a &= \frac{-C_{Y_\beta}}{4\mu_b \frac{b}{V}} + \frac{\lambda_1}{2} \\[2em]
\omega &= \sqrt{\frac{\left(K_X^2 C_{n_\beta} + K_{XZ} C_{l_\beta}\right)}{2\mu_b \left(\frac{b}{V}\right)^2 \left(K_X^2 K_Z^2 - K_{XZ}^2\right)}}
\end{aligned}\right\} \tag{4}$$
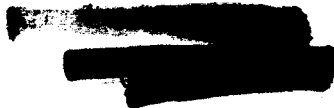
Roll-to-Sideslip Ratio

Simplified expressions which yield accurate values of the ϕ/β ratio for these altitudes when rotary derivatives are neglected can be determined.

For $\alpha = 0^\circ$ only the rolling-moment equation must be considered.

$$2\mu_b K_X^2 \lambda^2 \phi - C_{l_\beta} \beta = 0$$

or

$$\frac{\phi}{\beta} = \frac{C_{l_\beta}}{2\mu_b K_X^2 \lambda^2}$$

For the Dutch roll root, the real part is negligible in comparison with the imaginary part, and

$$\lambda^2 \approx \frac{-c_{n_\beta}}{2\mu_b K_Z^2}$$

Then

$$\frac{\phi}{\beta} \approx \frac{-K_Z^2}{K_X^2} \frac{c_{l_\beta}}{c_{n_\beta}} \tag{5}$$

For $\alpha = 16^o$, two equations must be considered because of principal-axis-inclination effect. A simple expression for ϕ/β results when the rolling- and yawing-moment equations are used:

$$2\mu_b K_X^2 \lambda^2 \phi - 2\mu_b K_{XZ} \lambda^2 \psi - c_{l_\beta}\beta = 0$$

$$-2\mu_b K_{XZ} \lambda^2 \phi + 2\mu_b K_Z^2 \lambda^2 \psi - c_{n_\beta}\beta = 0$$

from which

$$\frac{\phi}{\beta} = \frac{\left(K_Z^2 c_{l_\beta} + K_{XZ} c_{n_\beta}\right)}{\left(2\mu_b \lambda^2\right)\left(K_X^2 K_Z^2 - K_{XZ}^2\right)}$$

Again neglecting the real part of the Dutch roll root,

$$\lambda^2 \approx \frac{-\left(K_X^2 c_{n_\beta} + K_{XZ} c_{l_\beta}\right)}{2\mu_b \left(K_X^2 K_Z^2 - K_{XZ}^2\right)}$$

and

$$\frac{\phi}{\beta} \approx \frac{-\left(K_{XZ} c_{n_\beta} + K_Z^2 c_{l_\beta}\right)}{\left(K_X^2 c_{n_\beta} + K_{XZ} c_{l_\beta}\right)} \tag{6}$$

RESULTS AND DISCUSSION

Results are presented of stability-boundary plots, roots of characteristic equation, and roll-to-sideslip ratio to show lateral stability characteristics and of time histories of motions to show response characteristics and inertia coupling possibilities.

Stability-Boundary Plots

Stability-boundary plots were constructed to determine regions of oscillatory and aperiodic stability in terms of weathercock stability C_{n_β} and effective dihedral C_{l_β}. In the absence of aerodynamic-damping derivatives, the only aerodynamic characteristic contributing damping is C_{Y_β}. Figure 3 presents the results for two angles of attack, 0° and 16°, and two altitudes, 100,000 and 200,000 feet. The oscillatory boundary is the condition for neutral damping of the oscillation and is determined from Routh's discriminant (BC - AD = 0). On the cross-hatched side of the boundary the oscillation is unstable. The aperiodic boundary is the condition which exists when the aperiodic root is equal to zero and is defined by D (coefficient of characteristic equation) = 0. The cross-hatched side of this curve denotes a divergent aperiodic mode. The region of complete stability is located between the oscillatory and aperiodic boundaries. A thorough discussion of boundary plots is given in reference 1.

For an angle of attack of 0° (fig. 3(a)) and an altitude of 200,000 feet, the airplane has an unstable oscillation for positive effective dihedral except for a small stable region at small negative C_{l_β} values. For an altitude of 100,000 feet there is a large region of C_{n_β} and C_{l_β} values for which the airplane would be stable. As the angle of attack is increased to 16° (fig. 3(b)), the oscillatory boundary rotates clockwise for an altitude of 100,000 feet and the stable region takes in the whole first quadrant and a portion of the fourth quadrant (negative C_{n_β}). This shifting of the boundary is the expected effect of principal-axis inclination. For an altitude of 200,000 feet, inclination of the principal axis causes the oscillatory boundary to shift counterclockwise into the second quadrant. The difference in the effect of principal-axis inclination for the two altitudes is attributed to the term $C_W \cos \gamma \, K_{XZ} C_{n_\beta}$ in the D coefficient of equation (3). For an altitude of 200,000 feet the larger value (3.54) of C_W, the weight coefficient, causes this counterclockwise rotation of the oscillatory boundary.

The brakes-closed (configuration 1), brakes open (configuration 4), and the two intermediate brake configurations (configurations 2 and 3)

are located in figure 3 at the appropriate C_{n_β} and C_{l_β} values. The brakes-closed configuration is divergent at $\alpha = 0°$ but is completely stable at $\alpha = 16°$ as a result of principal-axis inclination. The brakes-open configuration at both angles of attack is completely stable at an altitude of 100,000 feet but has an unstable Dutch roll oscillation at an altitude of 200,000 feet.

Characteristic Roots

The roots of the characteristic equation were determined for the configurations indicated in figure 3 for altitudes of 100,000, 150,000, and 200,000 feet. The results are presented in table III as time to damp to one-half amplitude for both the Dutch roll and aperiodic modes and as period of oscillation for the Dutch roll mode.

The tabulated characteristics are in agreement with the qualitative results indicated by the stability-boundary plots. The aperiodic mode is always stable. The period of oscillation increases by a factor of 7 for an increase in altitude from 100,000 to 200,000 feet as a result of a decrease in dynamic pressure. The effect of changing the flight-path angle to -60° from 0° is negligible.

In figure 4, curves of constant period and damping of the Dutch roll oscillation are presented for angles of attack of 0° and 16° and an altitude of 100,000 feet in terms of weathercock stability and effective dihedral parameters. Although there are large regions of oscillatory stability for an altitude of 100,000 feet (fig. 3), the constant-damping curves of figure 4 show that the Dutch roll oscillation for both $\alpha = 0°$ and 16° is really only lightly damped throughout the region of normal values of C_{n_β} and C_{l_β}, that is, the first quadrant. For 200,000 feet, the airplane was shown in figure 3 to be unstable throughout the first quadrant except for very small values of effective dihedral for $\alpha = 0°$.

A few calculations have been made to determine the effect of rotary derivatives and constant pitching velocity on the characteristic modes. During flight at high altitudes the airplane will be in a ballistic flight path rather than in level flight and will experience a constant pitching velocity if angle of attack is held constant. For this condition pitching velocity influences lateral motion through inertia terms

$$2\mu_b \left(\frac{b}{V}\right)^2 \left(K_X^2 - K_Y^2\right)pq \quad \text{and} \quad 2\mu_b \left(\frac{b}{V}\right)^2 \left(K_Y^2 - K_Z^2\right)qr \quad \text{in the yawing- and}$$

rolling-moment equations, respectively. For a constant pitching velocity these terms act as equivalent C_{n_p} and C_{l_r} derivatives and were included in calculations of the roots for 100,000 and 150,000 feet. The results are included in table III where the C_{n_p} and C_{l_r} values denote this condition

of constant pitching velocity. For both altitudes the effect of constant
pitching velocity is to add an increment to the Dutch roll damping, a
decrement to the aperiodic mode, and to introduce a neutrally stable
aperiodic mode.

Two other calculations were made for altitudes of 100,000 and
200,000 feet in which estimates of the damping derivatives C_{n_r} and
C_{l_p} as well as the constant-pitching-velocity terms were included in
the equations of motion. For an altitude of 200,000 feet these additional
terms have a small effect on period and add an increment to Dutch roll
damping which is not significant, since the oscillation is only neutrally
stable at best. For 100,000 feet the period is unchanged, but the damping
of both the Dutch roll and damping-in-roll modes is appreciably increased
by including C_{n_r} and C_{l_p}. These results indicate that 100,000 feet
may not be a sufficiently high altitude for which damping derivatives can
be neglected. The effects of damping derivatives and constant pitching
on airplane responses will be discussed in a later section.

Roll-to-Sideslip Ratio ϕ/β

The ϕ/β ratio in the Dutch roll mode is an important flying quality
and has been calculated for the same configurations and conditions for
which roots were obtained. The ϕ/β ratios are given in table IV.
Although tolerable values of ϕ/β ratio are dependent on Dutch roll
damping, ϕ/β ratios greater than 4 have been found by pilots (ref. 2)
to be generally intolerable regardless of damping. From the table, it
is noted that angle of attack had a large favorable effect on the ϕ/β
ratio, the maximum value for $\alpha = 16°$ being 3.8 as compared with 15.9
for $\alpha = 0°$. This large reduction in ϕ/β is attributed to both a
reduction in C_{l_β} with increasing angle of attack and the effect of
principal-axis inclination as indicated by the approximate expression,
equation (6). Also, the ϕ/β ratio is practically independent of alti-
tude. For two cases in which constant pitching and constant pitching
plus C_{n_r} and C_{l_p} were considered, there was a negligible change in
ϕ/β ratios.

Time Histories

In flying the airplane in a high-altitude trajectory it was assumed
that the pilot would apply controls so that the airplane bank angle would
not exceed 90°. For this purpose the linear three-degree-of-freedom
lateral equations of motion were used with an analog computer to determine
airplane response to an initial sideslip angle, yawing-moment input, and
rolling-moment input for altitudes of 100,000 and 200,000 feet and angles

of attack of $0°$ and $16°$. In addition some five-degree-of-freedom motions
were also calculated to determine whether inertia coupling is a problem
at these speeds and altitudes. Time histories are shown for configura-
tions 1, 2, and 4.

Response to an initial sideslip angle.- The response to an initial
sideslip angle is presented in figure 5 for one intermediate brake con-
figuration to illustrate the oscillatory characteristics and roll-to-
sideslip ratio discussed previously. The curves show that the period at
200,000 feet is about seven times as great as the period at 100,000 feet
as discussed previously, the oscillation is more unstable at 200,000 feet,
and the ϕ/β ratio is about 15. Although the oscillation is more unstable
at 200,000 feet, as would be expected from the stability boundary plots,
it would appear to be easier to control because of the longer period.
Consequently, stability-boundary plots should not be relied upon solely
in appraising airplane stability characteristics since they do not provide
quantitative results. Response calculations provide valuable additional
information on the stability and control characteristics of the airplane.

Response to yawing-moment input.- Figure 6 presents the response
in bank and sideslip to a yawing-moment input for angles of attack of $0°$
and $16°$ and altitudes of 100,000 and 200,000 feet. The input is that
provided by the reaction control (equivalent to about $0.4°$ aerodynamic
control if no rolling moment is produced) for 100,000 feet and one-tenth
the reaction control (about $2°$ aerodynamic control) for 200,000 feet.
For $\alpha = 0°$, the brakes-closed configuration is unstable and the motions
are divergent. The other two configurations have small sideslip responses
at 100,000 feet but rapid roll responses as a result of dihedral effect
and the large dynamic pressure. At 200,000 feet, the sideslip motions
are larger and the roll responses are slower because of the greatly reduced
dynamic pressure. At $\alpha = 16°$, the brakes-closed configuration is stati-
cally stable and the roll response is slower than for $\alpha = 0°$ as a result
of principal-axis-inclination effect. The brakes-open configuration has
a very slow roll response at $\alpha = 16°$ because of the small value of
dihedral effect, C_{l_β}, shown in figure 3(b).

Response to rolling-moment input.- Figure 7 presents the responses
to a rolling-moment input for altitudes of 100,000 and 200,000 feet and
angles of attack of $0°$ and $16°$. The inputs were five times the rolling
moment provided by the reaction control or about $0.5°$ aileron deflection
(if no yawing moment is produced) for an altitude of 100,000 feet and a
rolling moment equal to the reaction control or about $5°$ aileron deflec-
tion for an altitude of 200,000 feet.

At $\alpha = 0°$, the brakes-closed configuration is unstable and the
motions are divergent. For large values of sideslip angle, the roll
direction is reversed by dihedral effect. At an altitude of 200,000 feet,
the roll reversal is not evident and would not occur until sideslip angles

become larger. The other configurations for $\alpha = 0°$ experience small sideslip angles and a rolling moment as expected.

At $\alpha = 16°$, the brakes-open configuration experiences a small sideslip motion and a rolling motion. The brakes-closed configuration is stable as a result of principal-axis inclination and the sideslip response is oscillatory. However, the roll is again reversed for this configuration at both altitudes as a result of negative C_{n_β}.

Recovery.- In figures 8 and 9, the effect on airplane motions of holding the control for 2 seconds and then neutralizing it is shown for both yawing- and rolling-moment inputs. When the control is neutralized, the airplane oscillates about a $0°$ sideslip angle but continues rolling in the absence of damping in roll. In order to stop the rolling, the aileron would have to be reversed to produce a roll acceleration of opposite sign.

Effect of rotary derivatives.- The effect of rotary derivatives and constant pitching terms on roots of characteristic equations has been discussed and was shown to be appreciable for an altitude of 100,000 feet. Since the Dutch roll and damping-in-roll modes experienced increases in damping it was desirable to determine the effect of these changes on airplane motions. A few calculations have been made for altitudes of 100,000 and 200,000 feet and $\alpha = 0°$ for the configuration having $C_{n_\beta} = 0.057$ and $C_{l_\beta} = -0.049$ to determine the effect of these derivatives on response to control inputs. For an altitude of 200,000 feet there were negligible changes in the motions.

In figure 10, the effect of rotary derivatives on the response in bank to a yawing-moment input is presented for an altitude of 100,000 feet. Terms included are the inertia-coupling terms introduced by the pitching velocity experienced in zero-lift flight (discussed in the section entitled "Characteristic Roots") and damping derivatives $C_{n_r} = -0.46$ and $C_{l_p} = -0.21$. The curves show a minor effect of rotary derivatives up to a bank angle of $-90°$. For maneuvers of longer duration, bank angles beyond $-90°$ in figure 10, the difference between the curves is appreciable, and it appears that in general rotary derivatives should be considered for altitudes up to 100,000 feet. However, rotary derivatives appeared to have a minor effect on the small motions presented in this paper.

Five-degrees-of-freedom results.- A few five-degree-of-freedom calculations have been made for configurations 2 and 4 for an angle of attack of $0°$ and an altitude of 100,000 feet. A range of yawing- and rolling-moment inputs varying from the magnitude of the reaction controls to several degrees of aerodynamic controls was considered to

determine the range of validity of the three-degree-of-freedom analysis and to investigate the inertia-coupling problem. In figure 11, results are presented for two configurations for which the inputs were a rolling moment 10 times as great as that provided by the reaction control, or about 1^O aileron deflection, and a yawing moment equal to that of the reaction control or about 0.4^O rudder deflection. Only for the intermediate brakes configuration and the yawing-moment input is there a considerable difference in sideslip response between the three-degree-of-freedom and the five-degree-of-freedom motions for these small inputs. The calculated critical rolling velocity for this configuration is 2 radians per second and at 2.8 seconds the airplane is experiencing this roll rate. At the critical roll rate, inertia-coupling terms in the equations are important, and hence the three-degree-of-freedom results are invalid. The significant result is that this intermediate brakes configuration $\left(\text{small } C_{n_\beta}\right)$ can experience roll-coupled motions at 100,000 feet for small yawing-moment inputs as a result of a high roll sensitivity to yaw controls.

Figure 12 presents results for the brakes-open configuration for inputs equivalent to 10° aileron deflection and 4° rudder deflection and initial angles of attack of 0°, 1^O, and 8°. The critical roll rate is about 4.4 radians per second and is a function of the pitch natural frequency for this configuration. Figure 12(a) presents the results for a rolling-moment input and illustrates the effect of the disturbance term $p\alpha$. For $\alpha_O = 0^O$, no coupled motions are evident even though critical roll rates are encountered. For $\alpha_O = 1^O$, some coupling is noted and for $\alpha_O = 8^O$ considerable motion in α and β is noted as the result of the large value of the $p\alpha$ term.

For the yawing-moment input (fig. 12(b)), more roll coupling is encountered for $\alpha_O = 0^O$ than for $\alpha_O = 8^O$. The roll rate did not approach the critical value for $\alpha_O = 8^O$ because of the small C_{l_β} at this α, which decreases the roll sensitivity to yawing-moment inputs.

Results for configuration 2 are presented in figure 13 for inputs of 10° aileron deflection and 4° rudder deflection. For the aileron input, no coupling effects are noted for an initial α of zero. For an initial α of 8° coupling effects are noted. However, the severity of the motions could not be determined because an angular velocity exceeded the range provided for in setting up the problem on an analog computer and caused the computer to overload before 1 second.

For the same reasons, the motions in response to 4° rudder input (fig. 13(b)) did not continue long enough to determine their forms. The sideslip response at $\alpha = 0^O$ appears to be divergent, but it is noted to be nothing more than a three-degree-of-freedom response to a rudder input. However, the rapid increase in α for this case indicates that roll coupling was probably present.

CONCLUSIONS

Results of an analytical investigation of the dynamic lateral stability characteristics of a configuration of the North American X-15 research airplane for a Mach number of 6.86 and altitudes of 100,000 and 200,000 feet, aerodynamic damping derivatives being neglected, indicate that

1. Roll-to-sideslip ratios were large at zero angle of attack because of large effective dihedral C_{l_β}.

2. Yawing-moment inputs produced large bank angles and roll rates at an altitude of 100,000 feet.

3. Although the brakes-closed configuration was stabilized by principal-axis inclination, its rolling characteristics are unsatisfactory in that dihedral effect reverses the roll direction.

4. Roll coupling developed from small rudder inputs at 100,000 feet for configurations having small weathercock stability C_{n_β} and large effective dihedral C_{l_β}.

5. The brakes-open configuration experienced roll coupling at 100,000 feet for both a $10°$ aileron input and a $4°$ rudder input.

6. The large roll-to-sideslip ratios ϕ/β, rolling sensitivity to yaw inputs, and roll coupling resulting from yaw inputs could be alleviated by reducing the effective dihedral C_{l_β}.

Langley Aeronautical Laboratory,
National Advisory Committee for Aeronautics,
Langley Field, Va., December 10, 1956.

NACA RM L56L27

REFERENCES

1. Sternfield, Leonard, and Gates, Ordway B., Jr.: A Simplified Method for the Determination and Analysis of the Neutral-Lateral-Oscillatory-Stability Boundary. NACA Rep. 943, 1949. (Supersedes NACA TN 1727.)

2. Williams, Walter C., and Phillips, William H.: Some Recent Research on the Handling Qualities of Airplanes. NACA RM H55L29a, 1956.

3. Phillips, William H.: Effect of Steady Rolling on Longitudinal and Directional Stability. NACA TN 1627, 1948.

TABLE I

GEOMETRIC AND INERTIA CHARACTERISTICS OF AIRPLANE

Wing:
  Area, sq ft 200
  Span, ft 22.36
  Mean aerodynamic chord, ft 10.27
Weight, lb 10,443
I_X, slug-ft^2 2,800
I_Y, slug-ft^2 50,000
I_Z, slug-ft^2 52,000
ϵ, deg 0

TABLE II

AERODYNAMIC SIDESLIP DERIVATIVES USED IN ANALYSIS

Configuration	$\alpha = 0^{\circ}$			$\alpha = 16^{\circ}$		
	C_{Y_β}	C_{n_β}	C_{l_β}	C_{Y_β}	C_{n_β}	C_{l_β}
1 (brakes closed)	-0.61	-0.043	-0.029	-0.72	-0.006	-0.046
2	-.74	.057	-.049	-.78	.038	-.039
3	-.89	.171	-.073	-.84	.089	-.032
4 (brakes open 45°)	-1.32	.487	-.137	-1.03	.229	-.011

TABLE III

CHARACTERISTIC MODES OF LATERAL MOTION

Configuration	Altitude, ft	α, deg	γ, deg	Aperiodic mode $T_{1/2}$, sec	Dutch roll $T_{1/2}$, sec	Dutch roll P, sec
(C_{n_p} = 0.037, C_{l_r} = 0.004) C_{n_r} = -0.46, C_{n_p} = 0.037, C_{l_r} = 0.004) C_{l_p} = -0.21	100,000 →	0 → 16 →	0 → -60 → -60	0.41, -0.43, -11.9; 9.3, 44	----, -56, 39	----, 3.3, 3.3
				∞; 81, 1.7; 18.8; 29; 16.8; 43	16.4, 61, 22, ∞, 19.3	3.3, 1.9, 1.1, 3.3, 1.1
(C_{n_p} = 0.31, C_{l_r} = 0.03)	100,000 →	0 → 16 →	0 → -60 → -60	39, 47, 55, 69, 61, 77	47, 38, 32, 24, 35, 23	1.8, 1.5, 1.3, 1.0, 1.5, 1.0
	150,000 →	0 → 16 →	0 → 0 →	1.1, -1.2, -12.9; 10.3, 69	----, -23, ∞	----, 9.1, 9.1
			-60 -60	∞, 69; 31.1, 43, 52, 76	∞, ∞, ∞, ∞	3.1, 4.9, 2.8, 2.8
(C_{l_p} = -0.21, C_{n_p} = 2.0, C_{n_r} = -0.46, C_{l_r} = 0.20)	200,000 →	0 → 16 →	0 → -60 -60	2.7, -3.5, -11.5; 10.3, 47.5	----, -21, ∞	----, 23, 24
				∞, 47.5; 19.7, 30, 17.9, 45	-41, -64, -37, ∞	13.5, 8.0, 23, 8.0
	200,000 →	16 →	0 → -60 -60	41, 50, 57, 72, 64, 80	-86, ∞, ∞, ∞, ∞, ∞	12.5, 10.8, 9.4, 7.3, 10.8, 7.3

TABLE IV

ROLL-TO-SIDESLIP RATIO IN DUTCH ROLL MODE

Configuration	α, deg	γ, deg	ϕ/β at altitude, ft, of — 100,000	150,000	200,000
1	0	0	Divergent 15.9	Divergent 15.8	Divergent 15.0
2		0	----	15.9	----
2 $(C_{n_p} = 0.31,\ C_{l_r} = 0.03)$			16.2	----	----
2 $(C_{l_p} = -0.21,\ C_{n_r} = -0.46,\ C_{n_p} = 0.037,\ C_{l_r} = 0.004)$			7.9	----	7.9
3			5.2	----	5.2
4			15.9	----	15.5
2		-60	5.2	----	5.2
4		-60	----	----	----
1	16	0	3.8	3.8	3.8
2		0	3.1	3.1	3.1
3			2.7	----	2.7
4			2.1	2.1	2.1
2		-60	3.1	----	3.1
4		-60	2.1	----	2.1

Figure 1.- Three-view drawing of airplane. All dimensions are in inches.

C_{Y_β}, 1/rad.

C_{n_β}, 1/rad.

—————— BRAKES RETRACTED
– – – – –   "   EXTENDED 45°

C_{l_β}, 1/rad.

α, deg
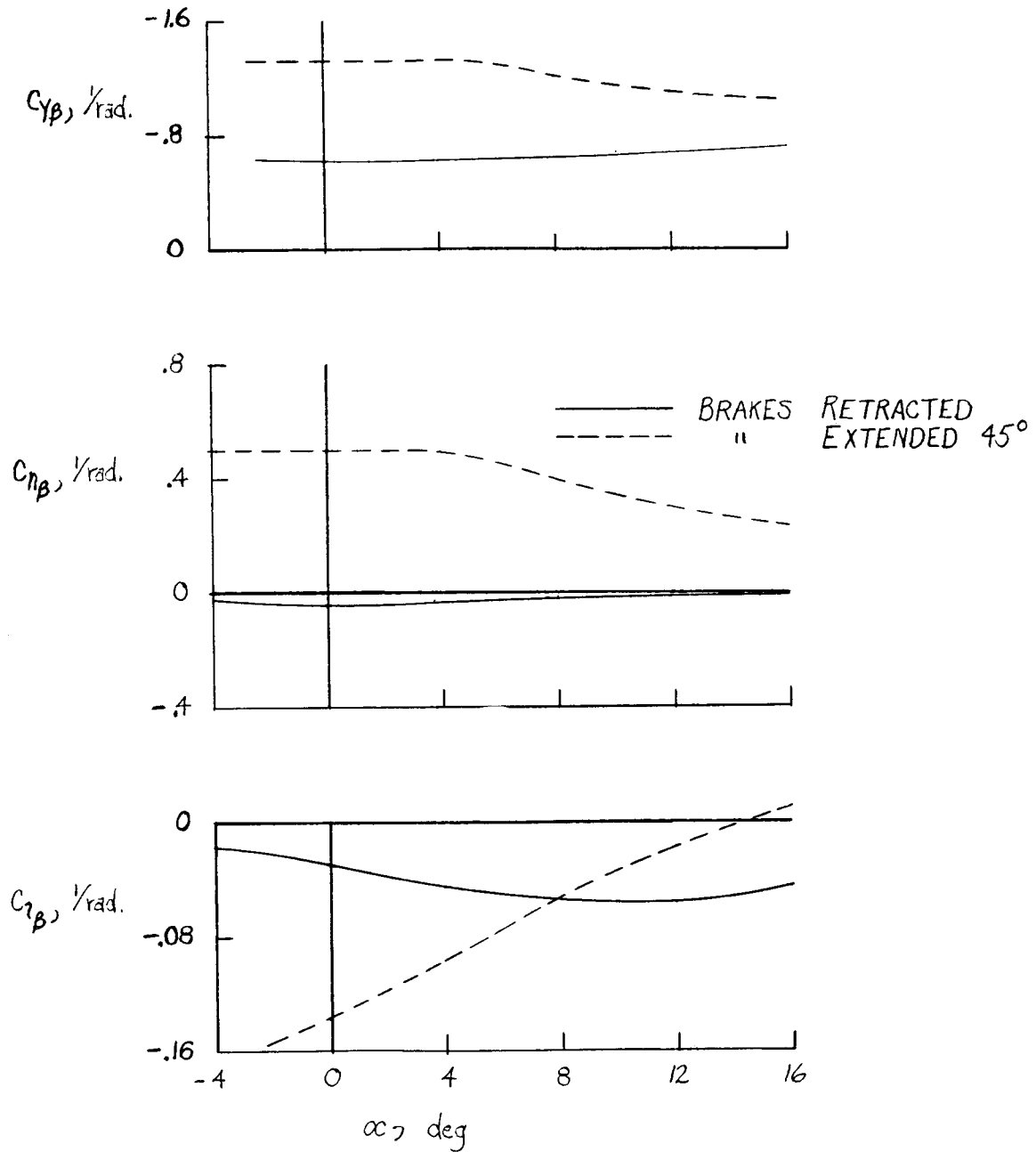
Figure 2.- Experimental data obtained in Langley 11-inch hypersonic tunnel.
M = 6.86.
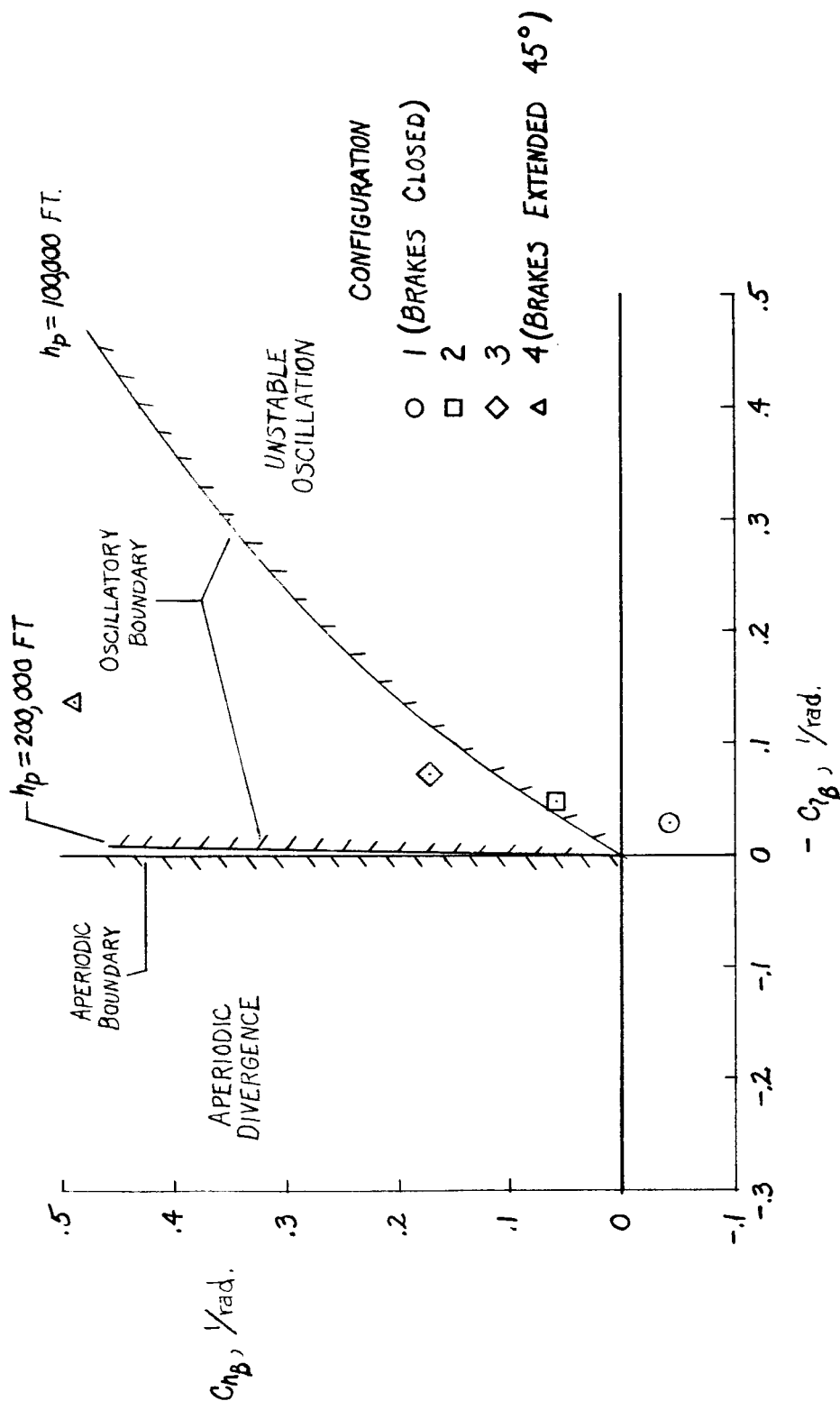
Figure 3.- Plot of lateral stability boundary.

(a) $\alpha = 0°$.
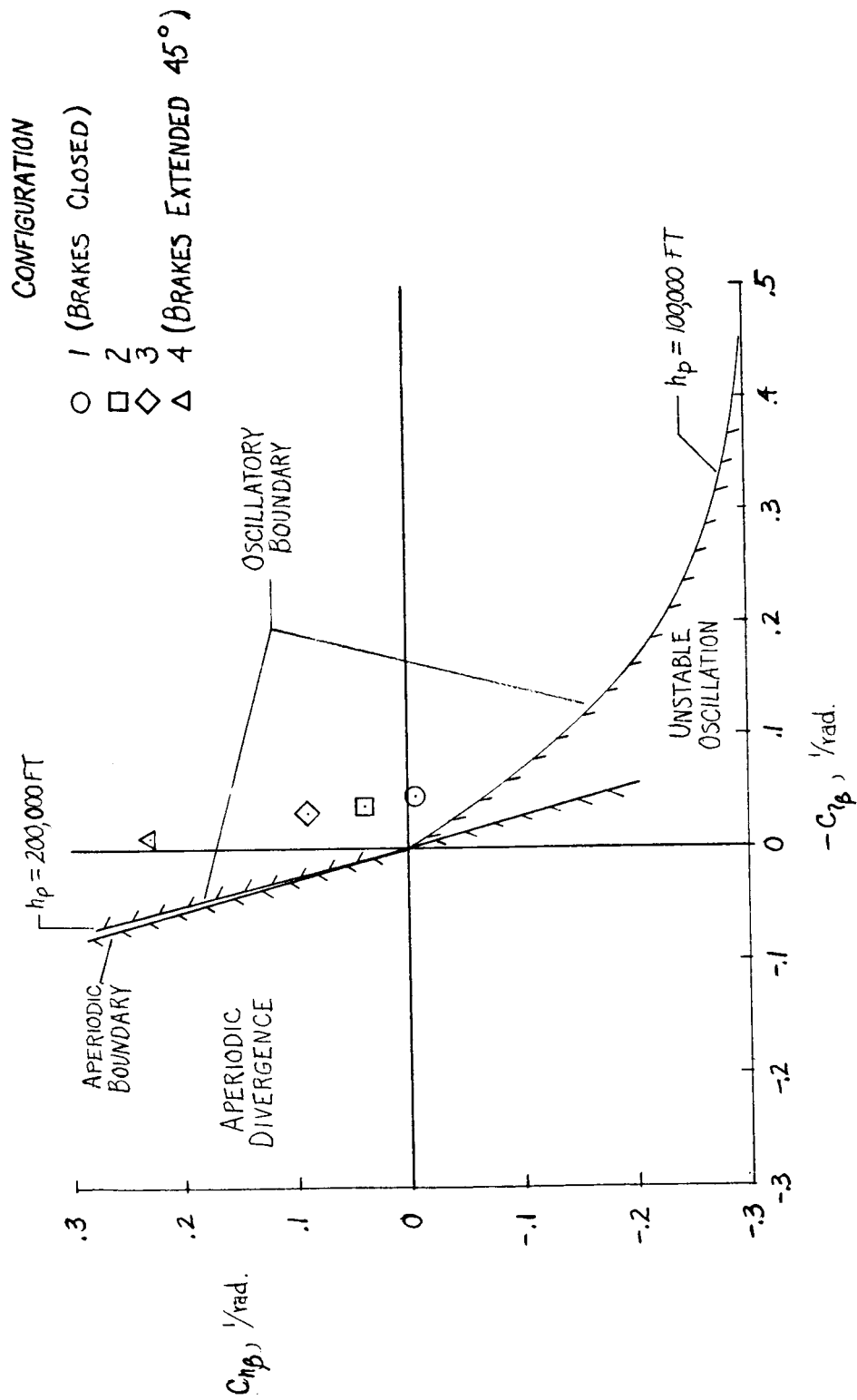
(b) α = 16°.

Figure 3.- Concluded.

PERIOD, SEC.

$T_{1/2}$ =

$-C_{l_\beta}$, 1/rad,

C_{n_β}, 1/rad
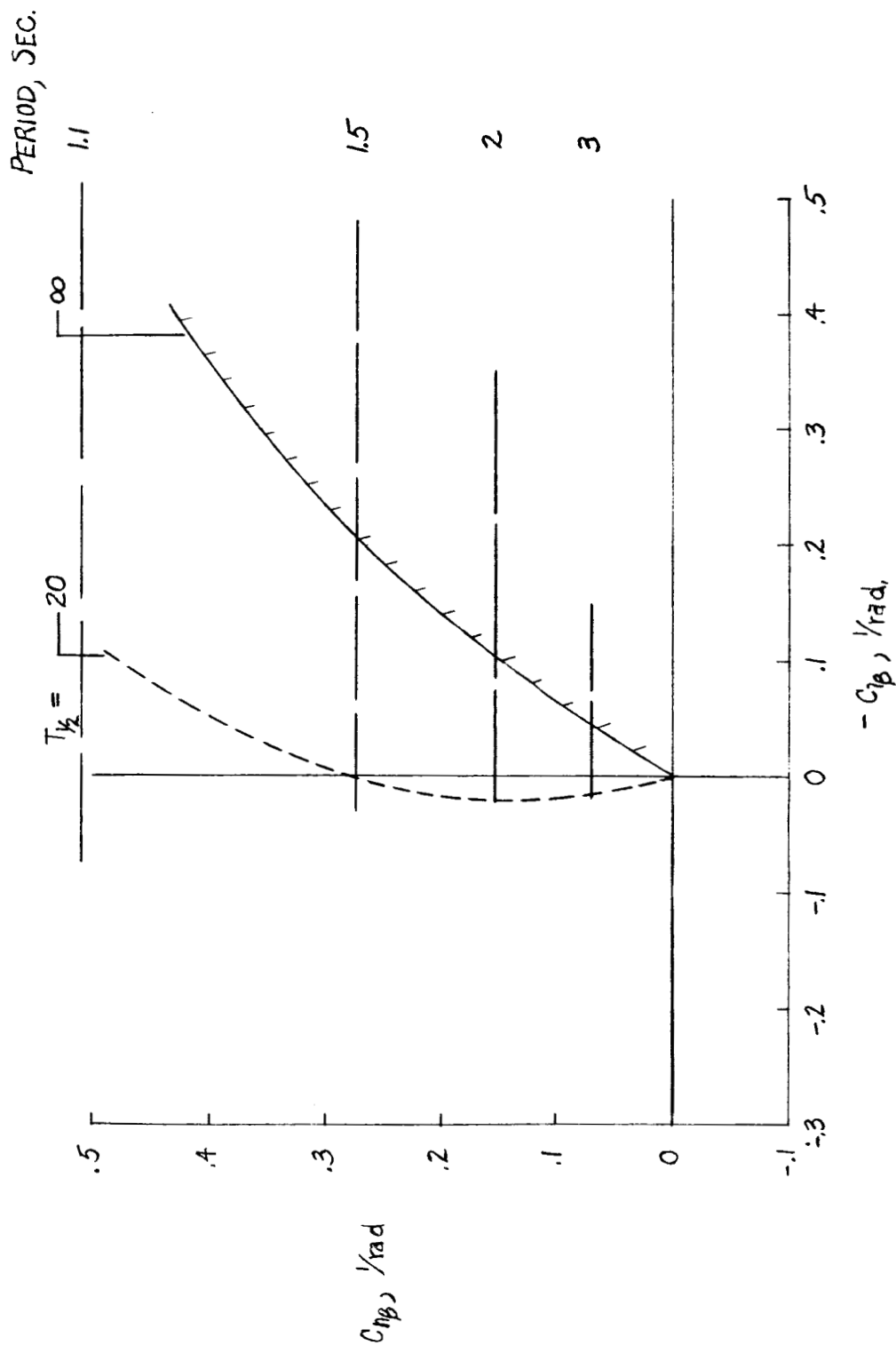
(a) $\alpha = 0°$.

Figure 4.- Curves of constant period and damping for Dutch roll oscillation. $h_p = 100,000$ ft.
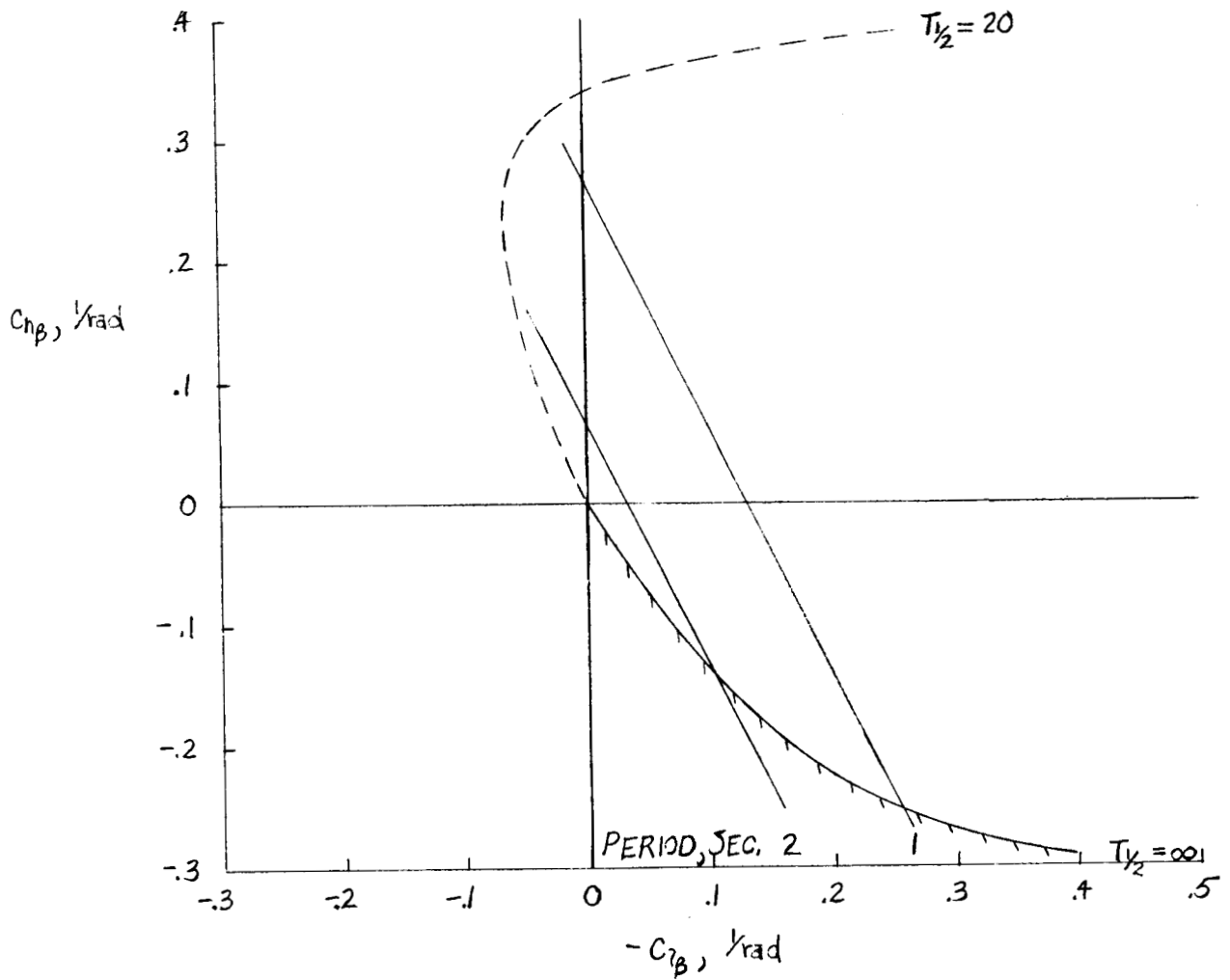
(b) $\alpha = 16°$.

Figure 4.- Concluded.
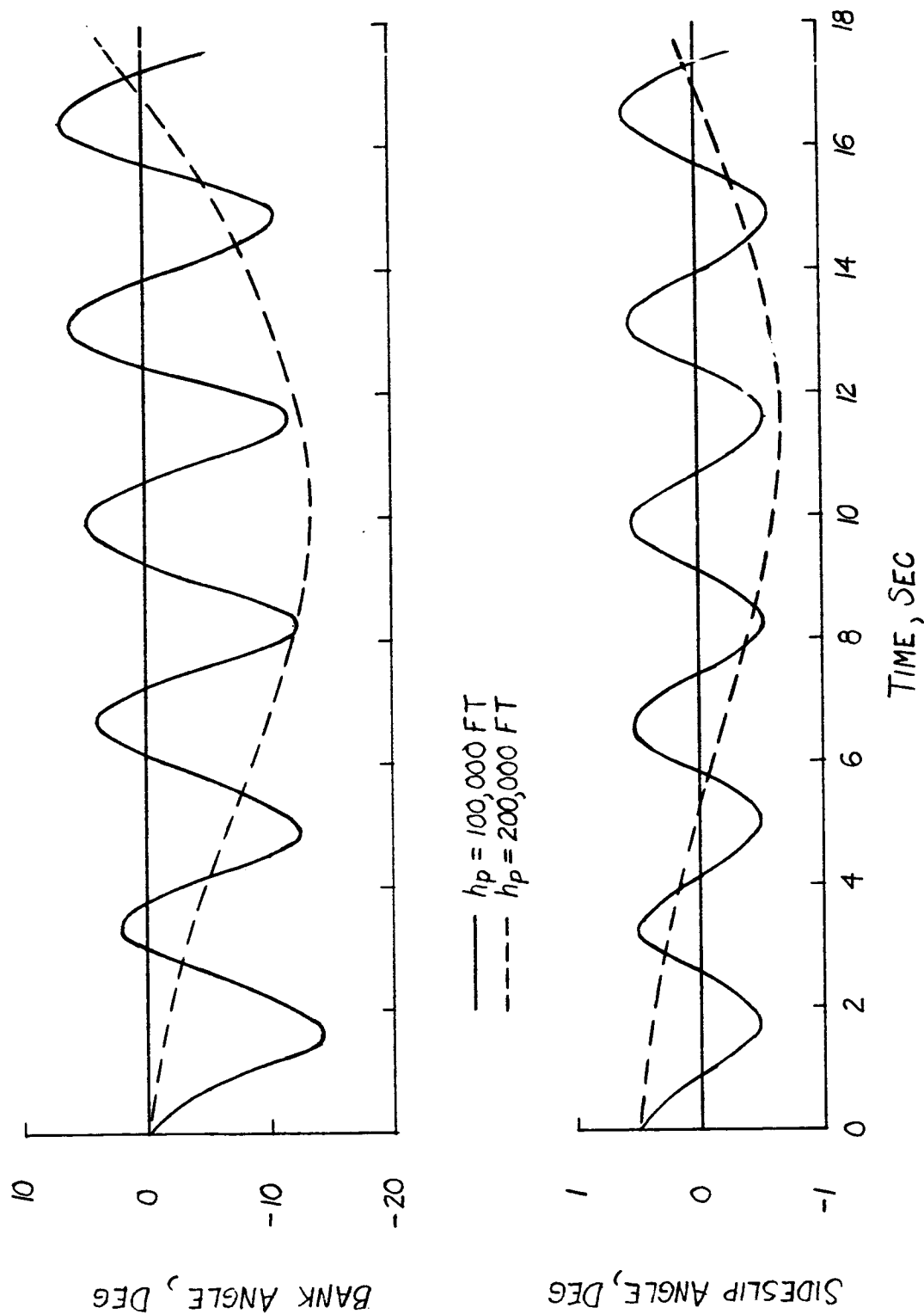
Figure 5.- Response to initial sideslip angle. Configuration 2; $\alpha = 0°$.
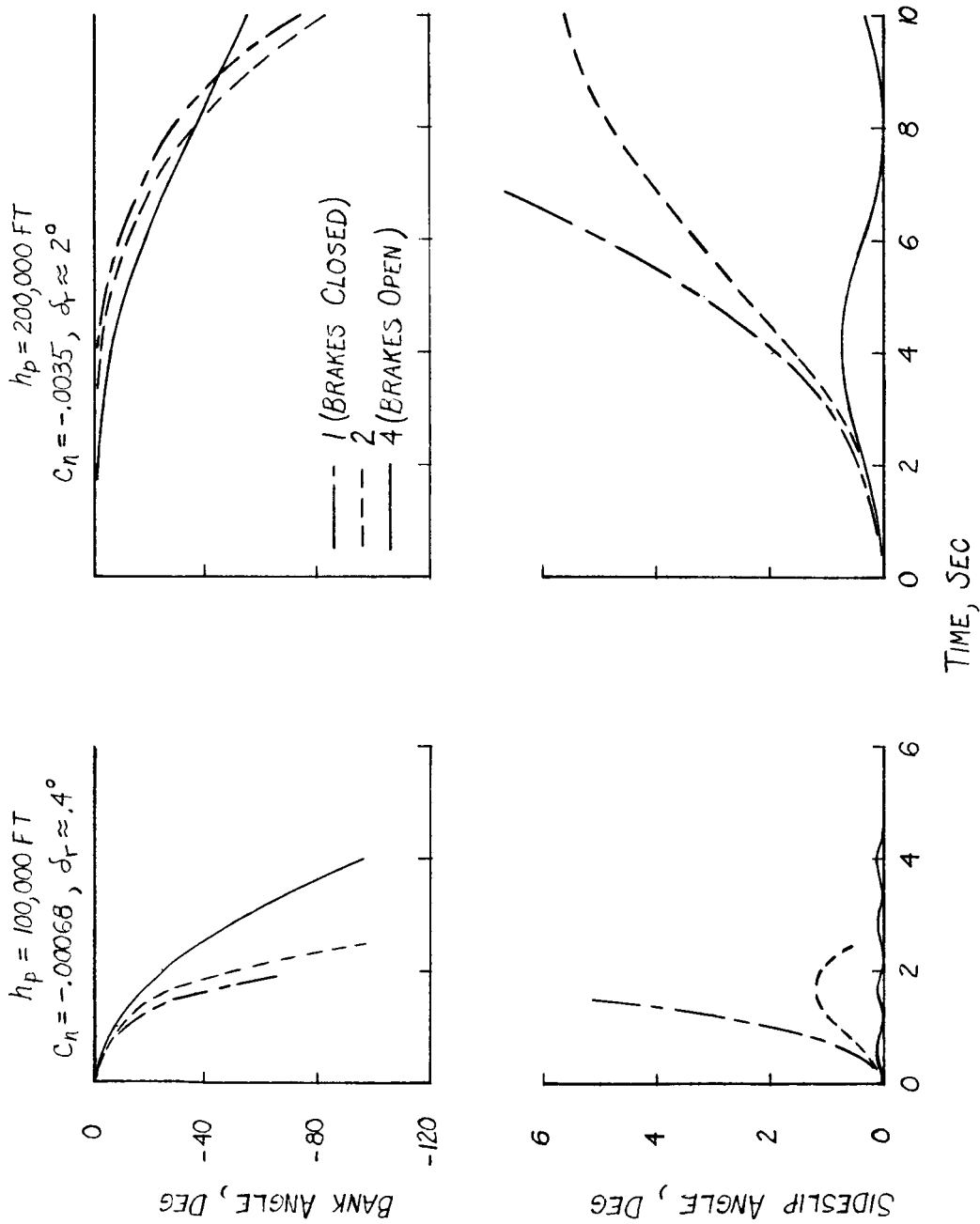
(a) α = 0°.

Figure 6.- Response to yawing moment.

DECLASSIFIED
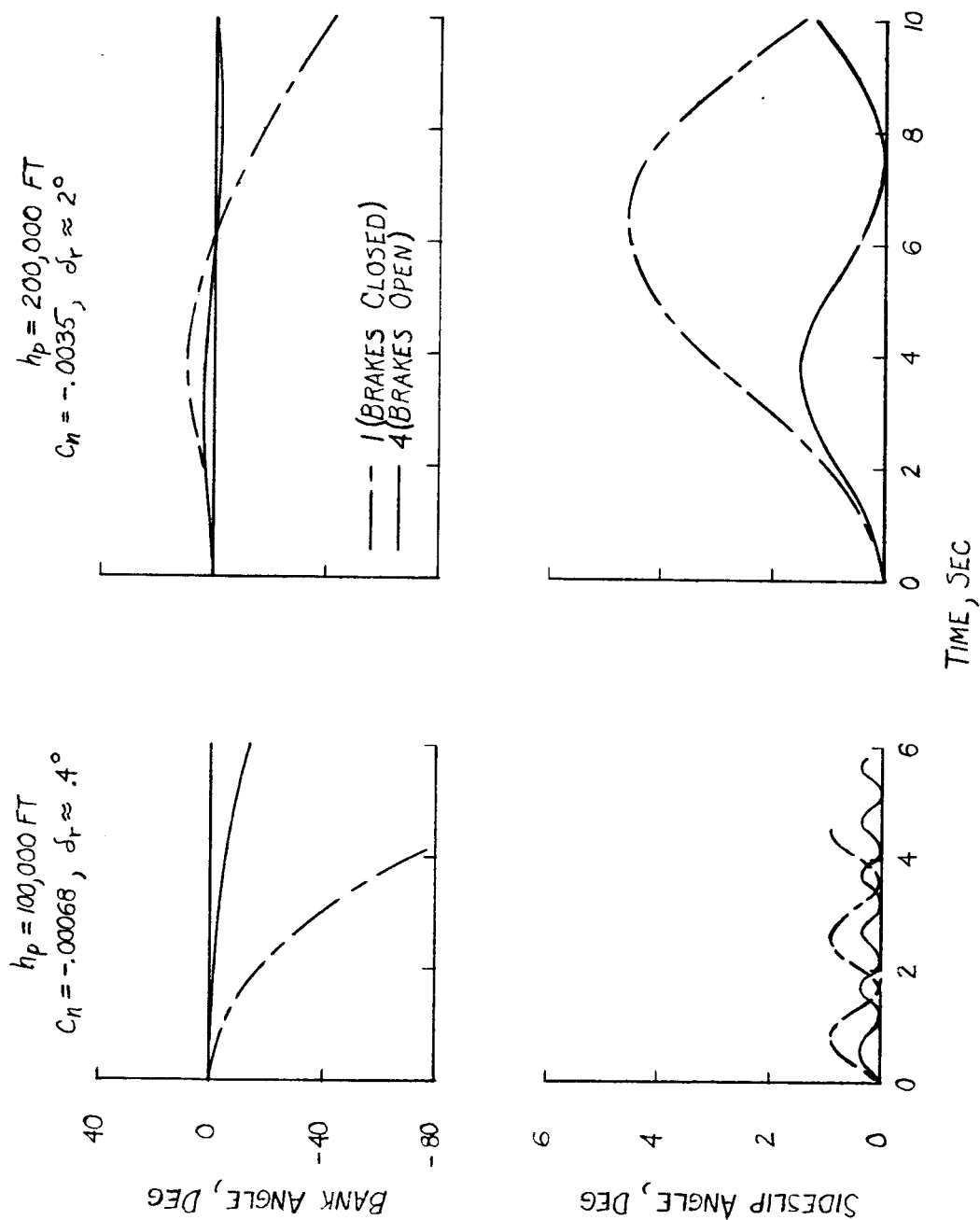
(b) $\alpha = 16°$.

Figure 6.- Concluded.
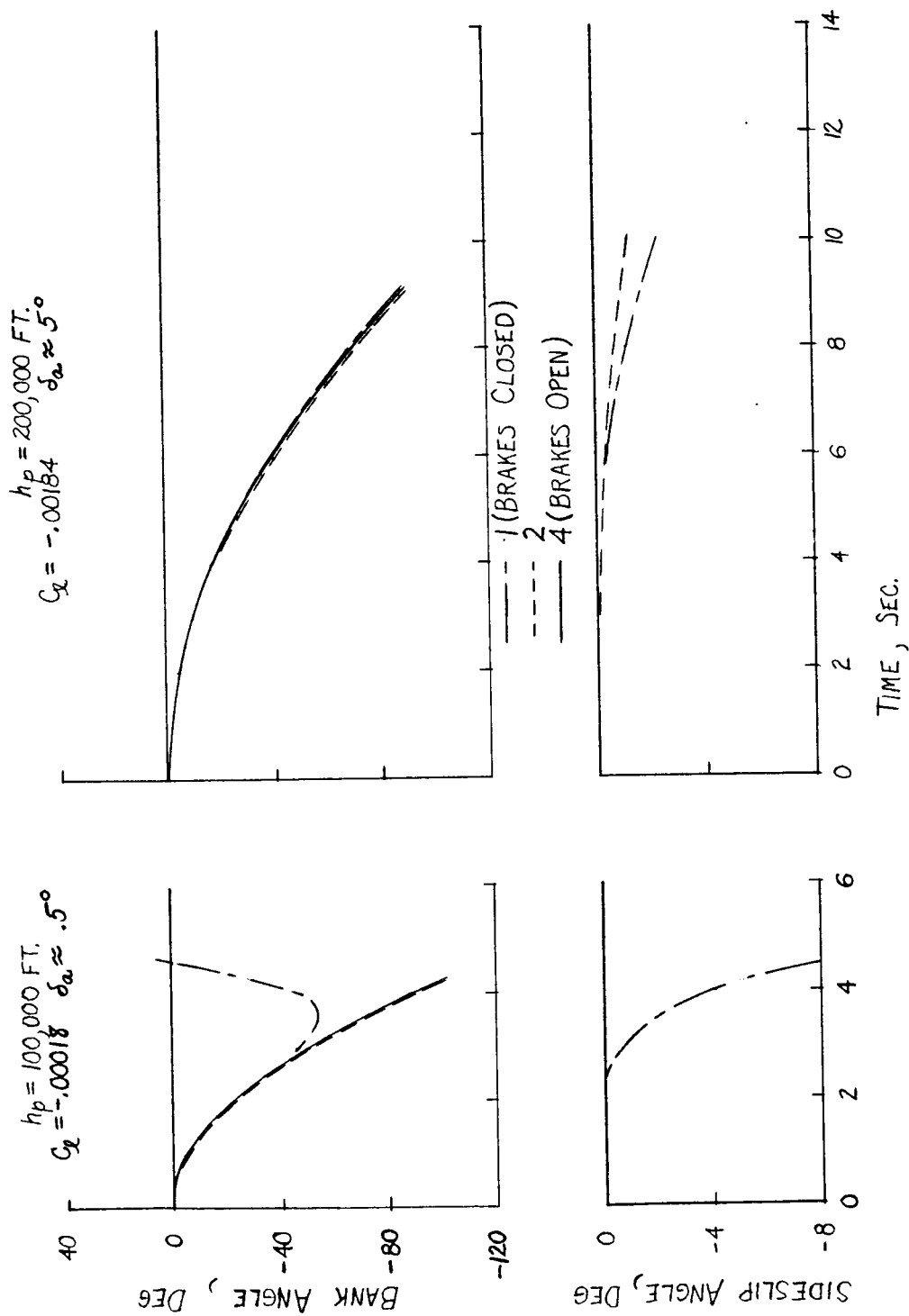
Figure 7.- Response to rolling moment.
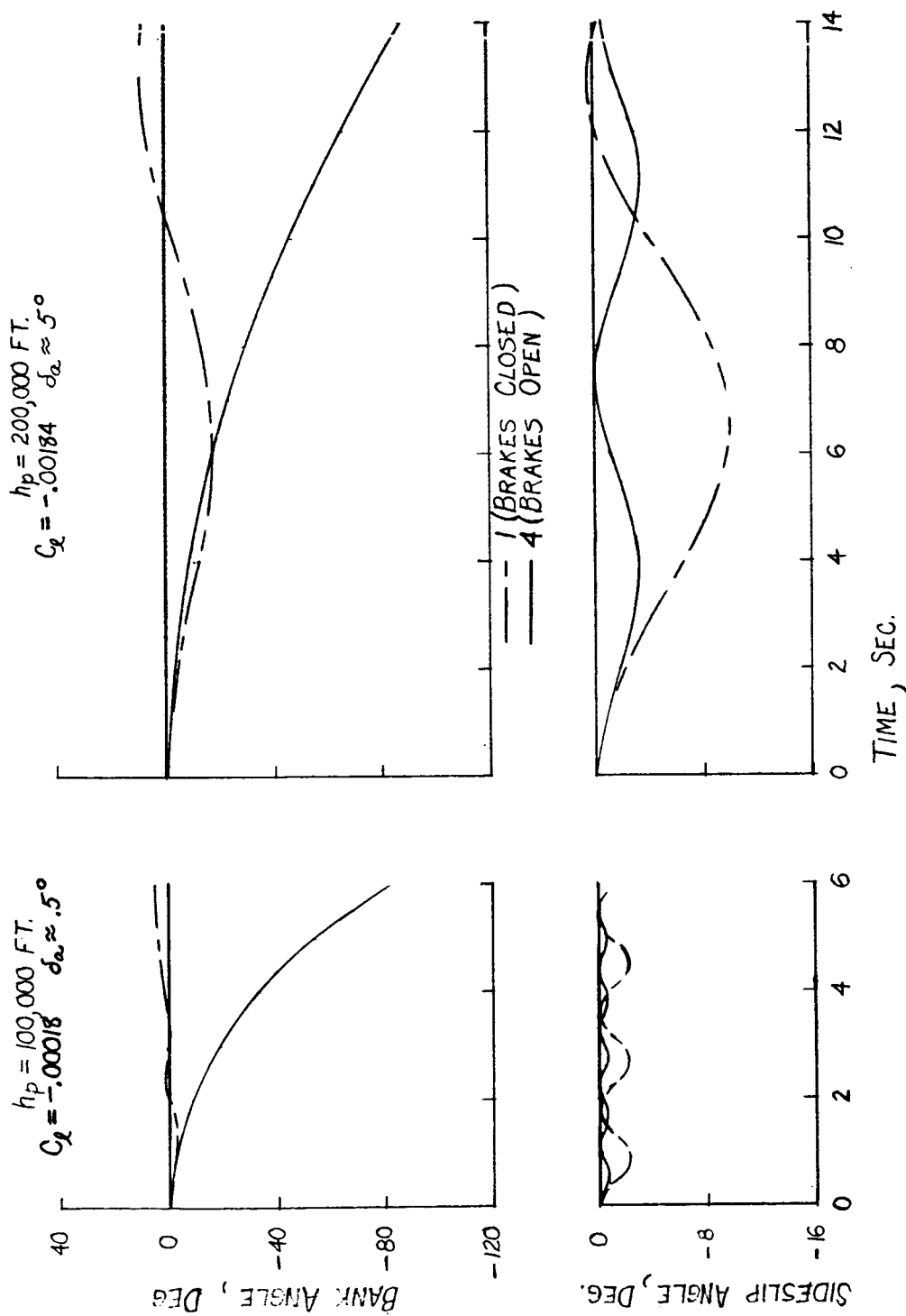
(b) $\alpha = 16^{\circ}$.

Figure 7.- Concluded.
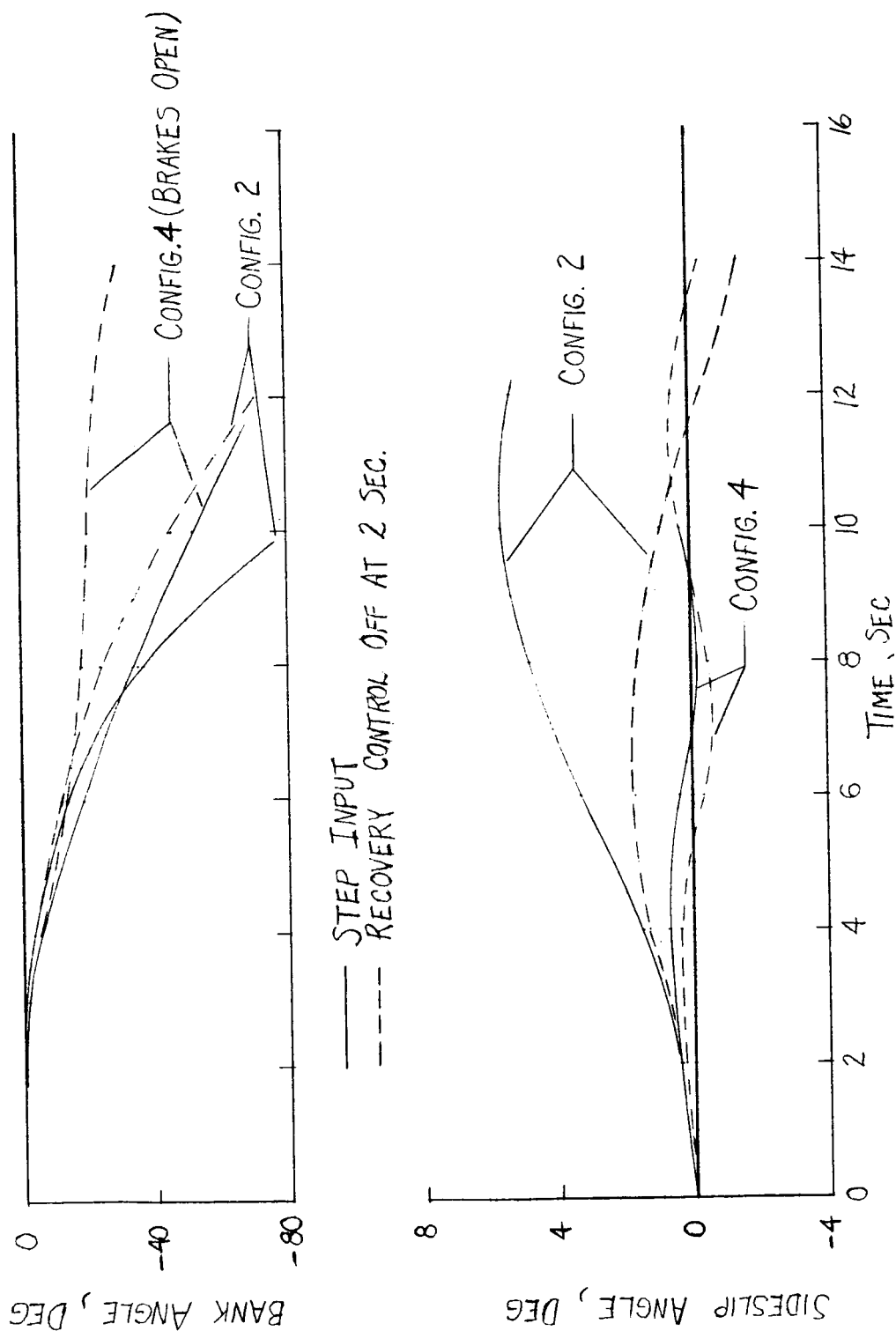
Figure 8.- Yawing moment responses with recovery. h_p = 200,000 ft; α = 0°; C_n = -0.0035; $\delta_r \approx 2°$.
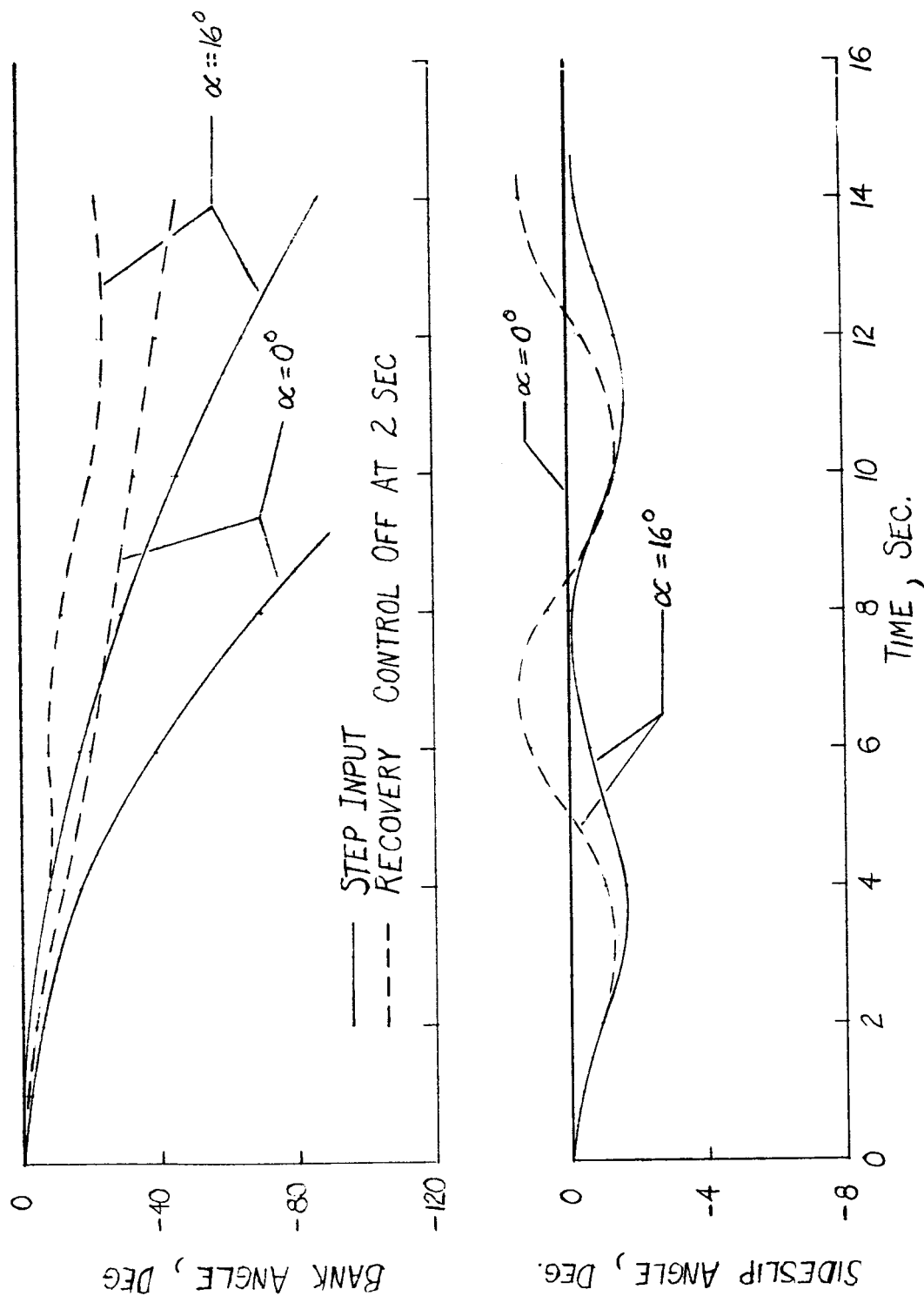
Figure 9.- Rolling moment response of configuration 4 (brakes open) with recovery. h_p = 200,000 ft; C_l = -0.00184; $\delta_a \approx 5°$.
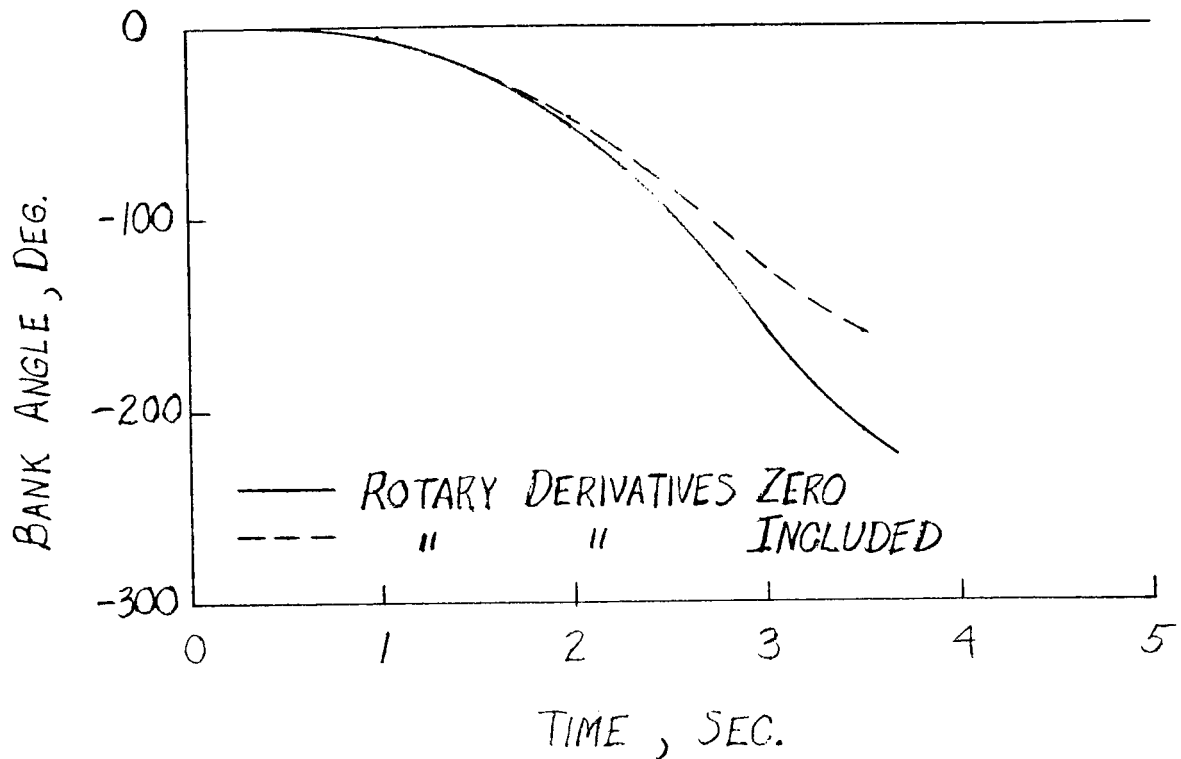
Figure 10.- Effect of rotary derivatives on response to yawing moment of configuration 2. $h_p = 100,000$ ft; $\alpha = 0^\circ$; $C_n = -0.00068$; $\delta_r \approx 0.4^\circ$.
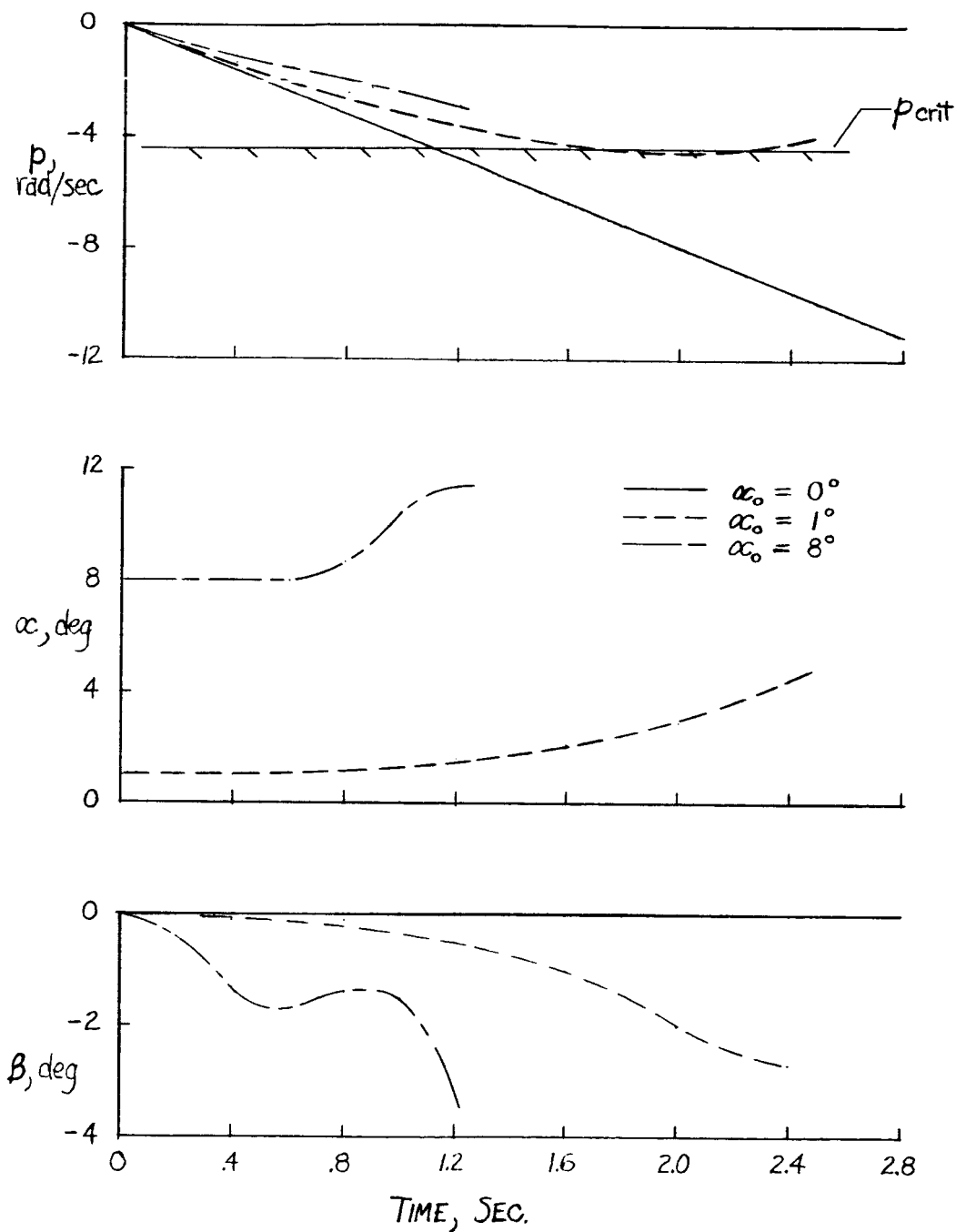
DECLASSIFIED

$C_l = -0.00036$ $\delta_a \approx 1°$

FIVE DEG. OF FREEDOM
THREE DEG. OF FREEDOM

$C_n = -0.00068$ $\delta_r \approx 0.4°$
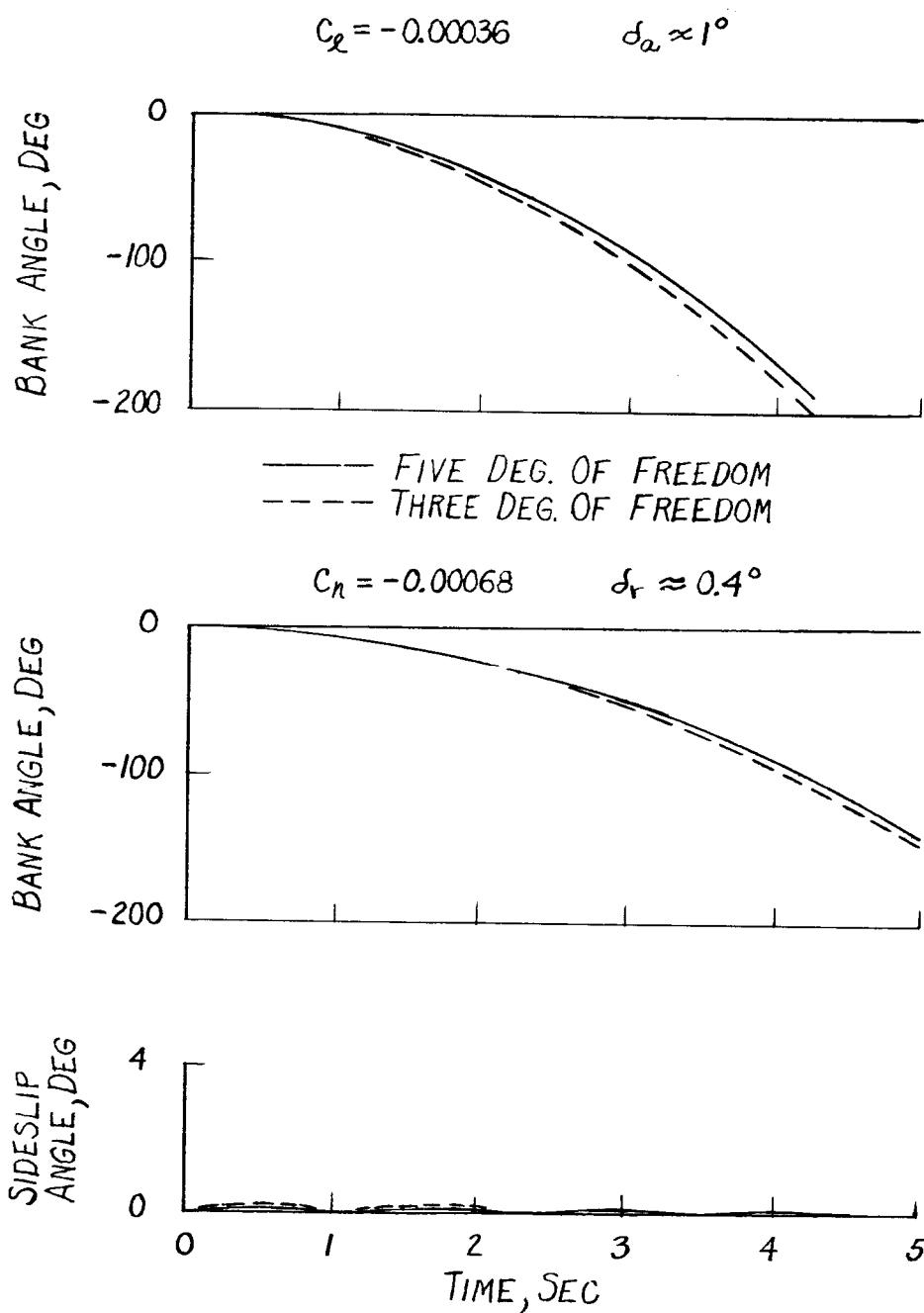
(a) Configuration 4, brakes open.

Figure 11.- Comparison of three- and five-degree-of-freedom responses. $h_p = 100,000$ ft; $\alpha = 0°$.

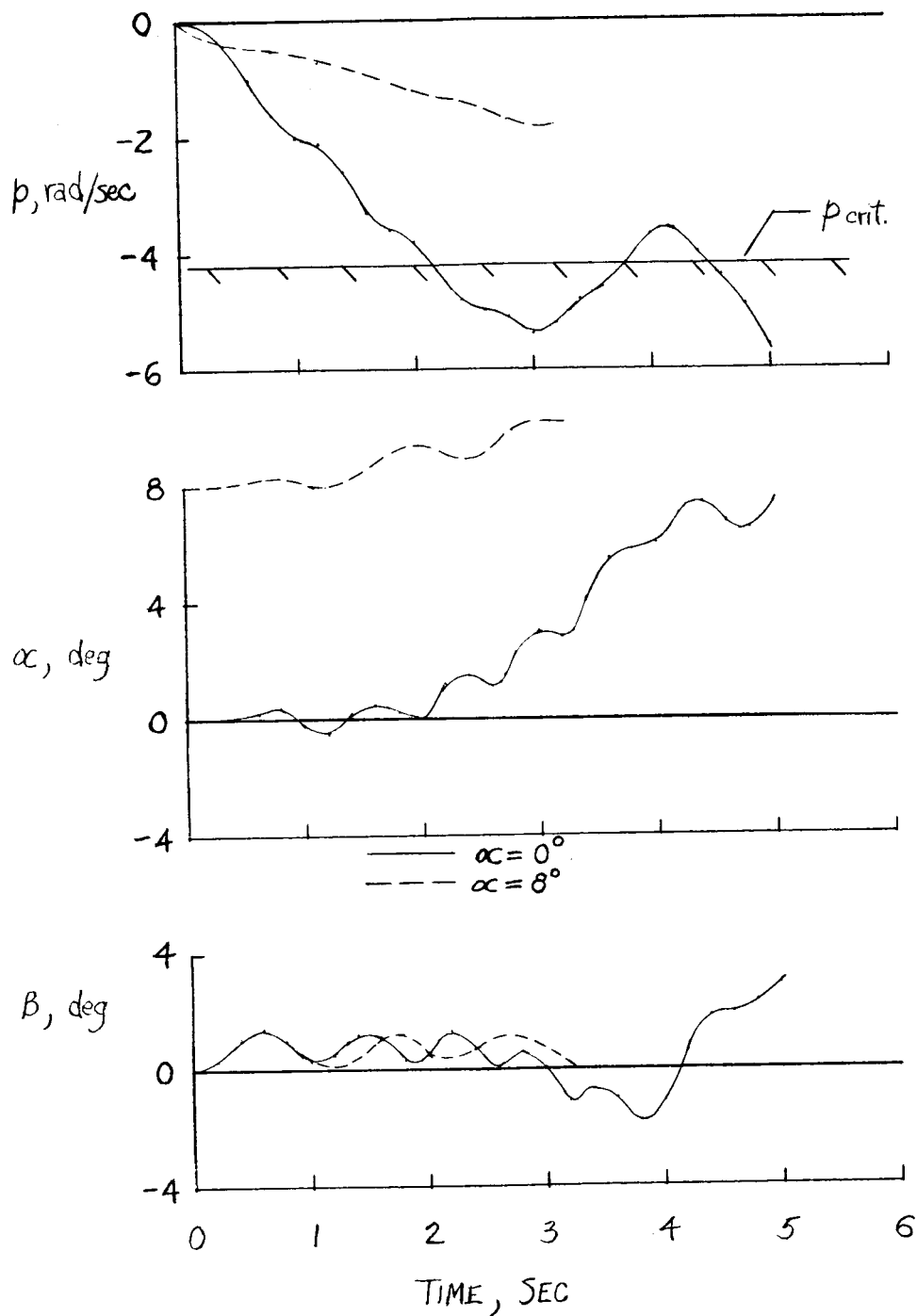$C_\ell = -.00036$ $\delta_a \approx 1°$

FIVE DEG. OF FREEDOM
THREE " " "
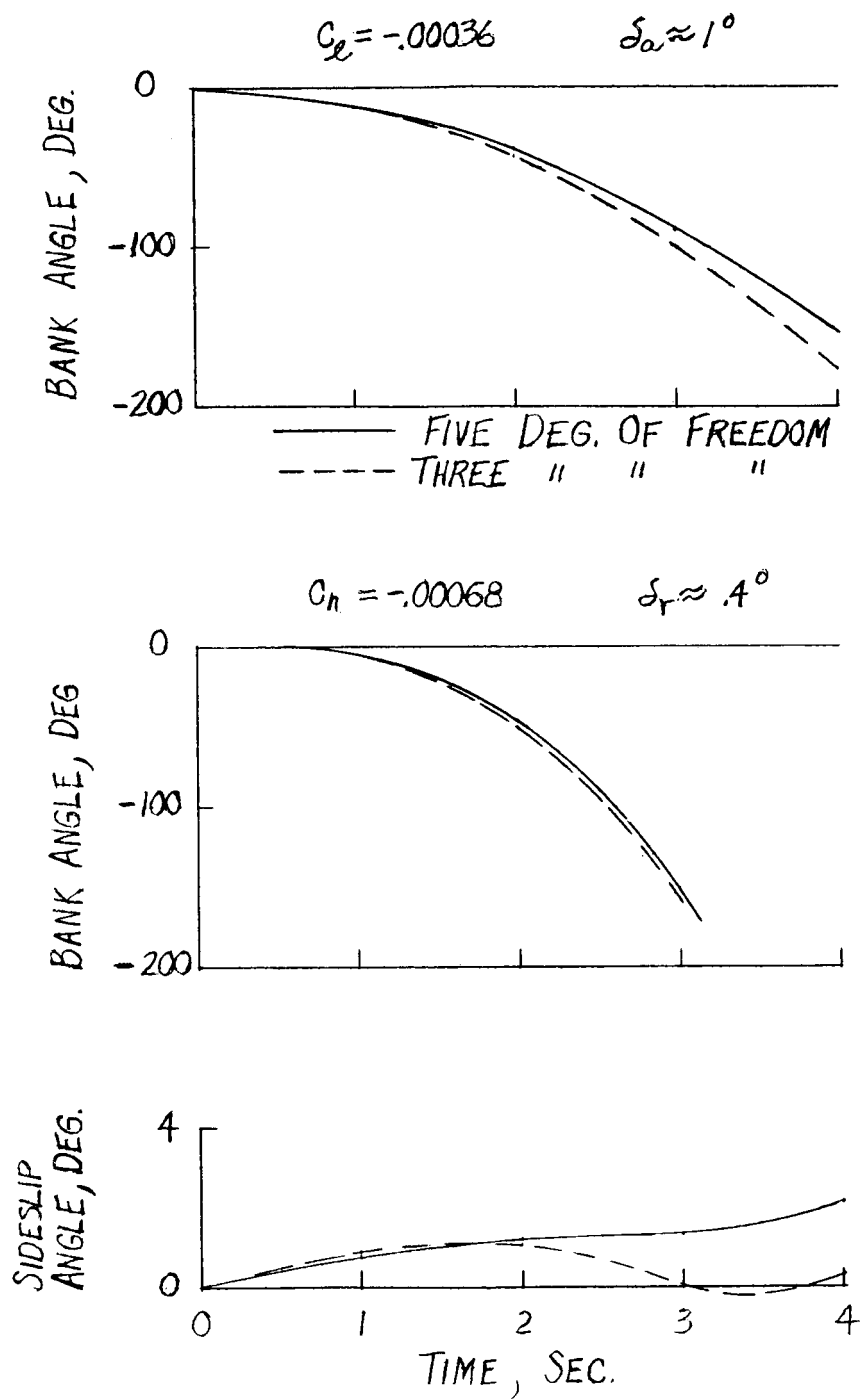
$C_n = -.00068$ $\delta_r \approx .4°$
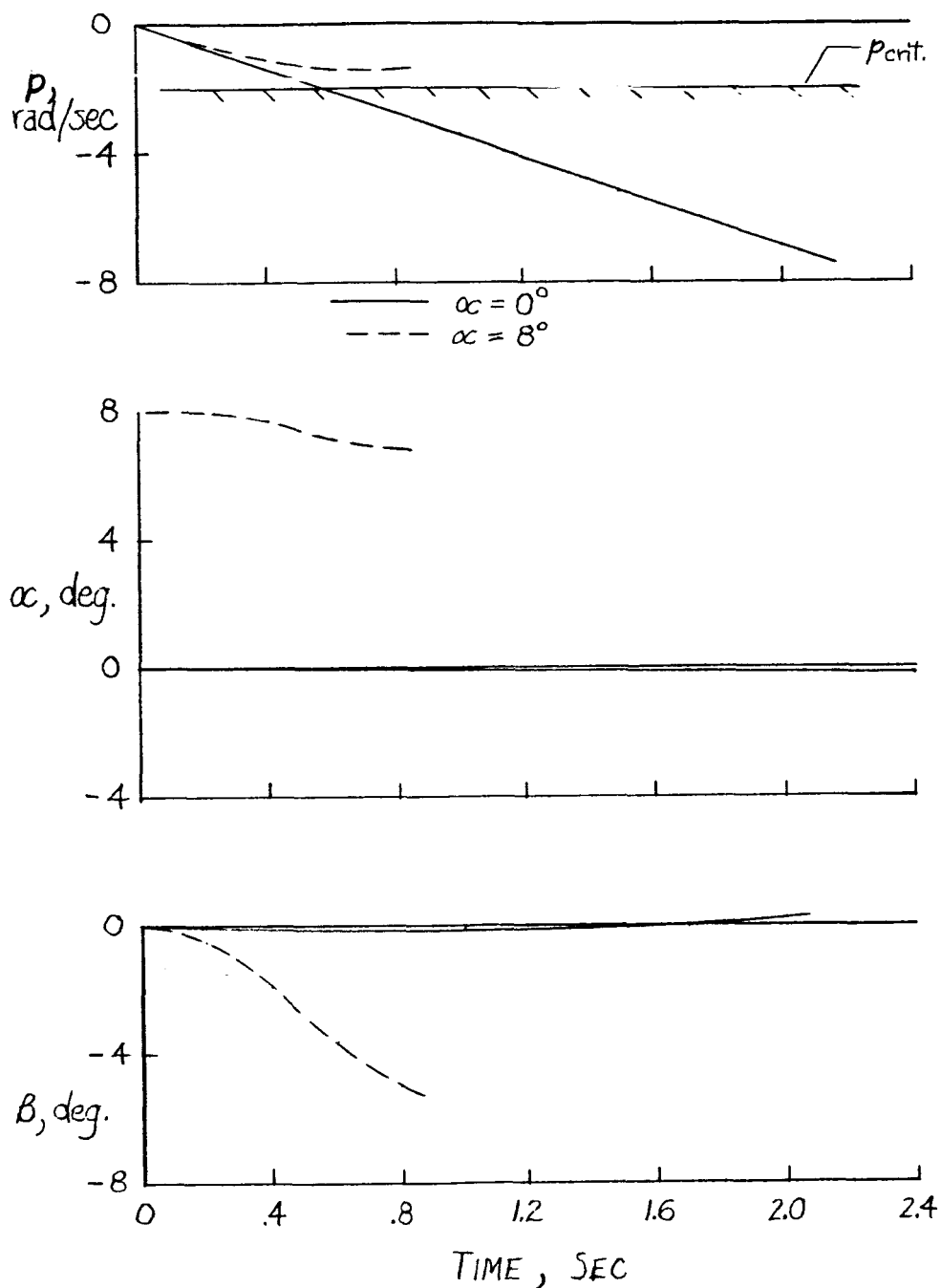
(b) Configuration 2.

Figure 11.- Concluded.

(a) Response to rolling moment. C_l = -0.0036; $\delta_a \approx 10°$.

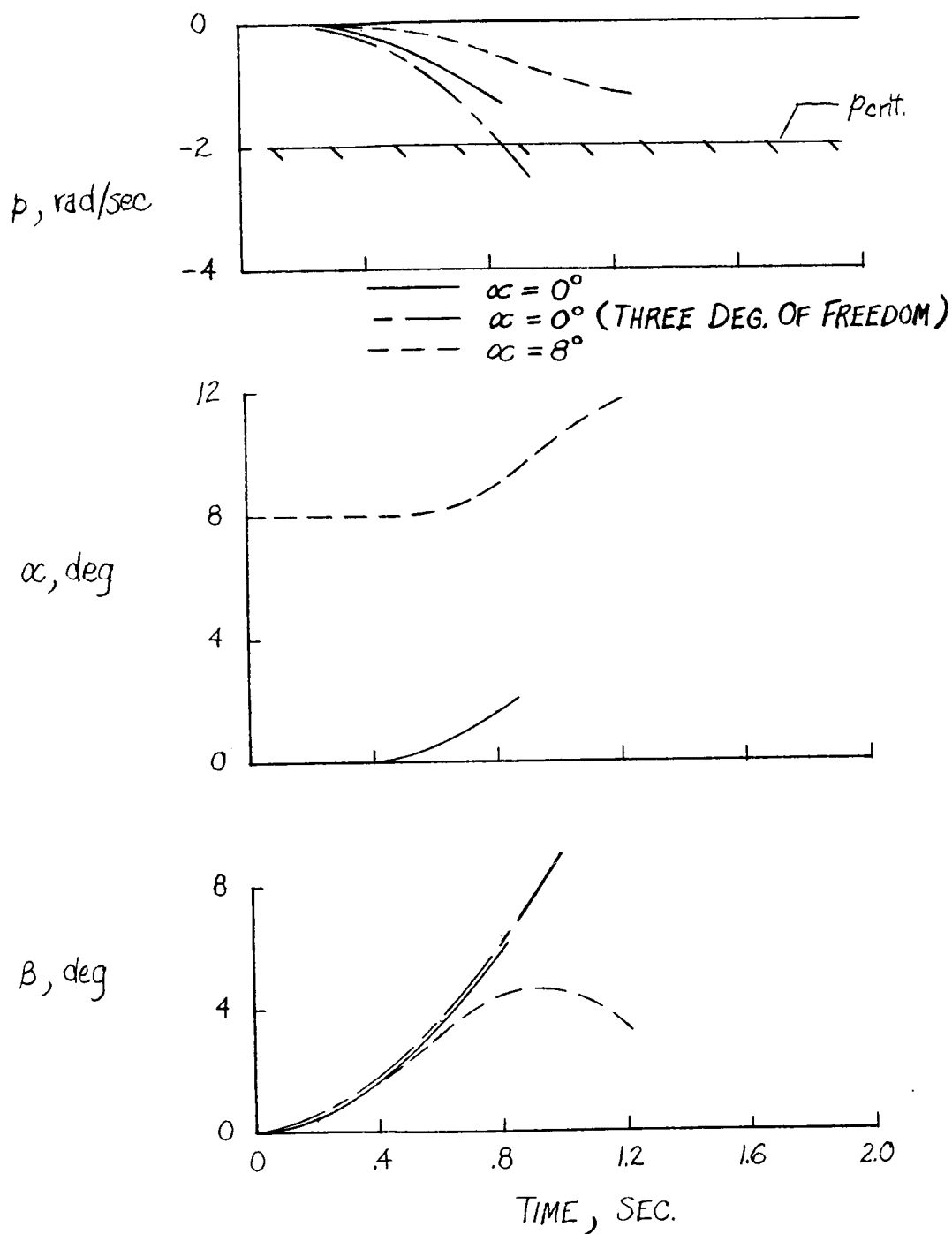Figure 12.- Five-degree-of-freedom results for configuration 4 (brakes open). h_p = 100,000 ft.

(b) Response to yawing moment. $C_n = -0.0068$; $\delta_r \approx 4°$.

Figure 12.- Concluded.

(a) Response to rolling moment. $C_l = -0.0036$; $\delta_a \approx 10^\circ$.

Figure 13.- Five-degree-of-freedom results for configuration 2.
$h_p = 100,000$ ft.

(b) Response to yawing moment. $C_n = -0.0068$; $\delta_r \approx 4°$.

Figure 13.- Concluded.